Acta Crystallographica Section F
Structural Biology and Crystallization Communications
ISSN 1744-3091

Crystallization and preliminary X-ray diffraction analysis of a tRNA^{Ser} acceptor-stem microhelix

Charlotte Förster,[a] Norbert Krauss,[b] Arnd B. E. Brauer,[a] Karol Szkaradkiewicz,[a] Svenja Brode,[a] Klaus Hennig,[a] Jens P. Fürste,[a] Markus Perbandt,[c] Christian Betzel[c] and Volker A. Erdmann[a]*

[a]Institute of Chemistry and Biochemistry, Free University Berlin, Thielallee 63, 14195 Berlin, Germany, [b]Charité Medical School of Berlin, Institute of Biochemistry, Protein Structure Research Group, Campus Charité-Mitte, Monbijoustrasse 2, 10117 Berlin, Germany, and [c]Institute of Biochemistry and Food Chemistry, University of Hamburg, c/o DESY, Notkestrasse 85, Building 22a, 22603 Hamburg, Germany

Correspondence e-mail: erdmann@chemie.fu-berlin.de

Received 27 March 2006
Accepted 4 May 2006

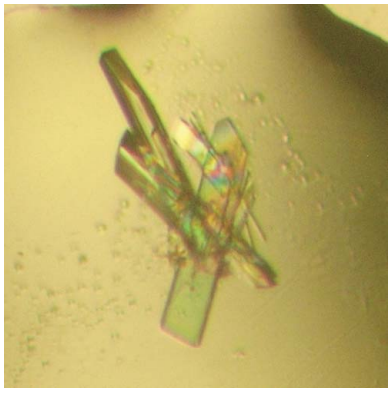

In order to understand elongator tRNA^{Ser} and suppressor tRNA^{Sec} identity elements, the respective acceptor-stem helices have been synthesized and crystallized in order to analyse and compare their structures in detail at high resolution. The synthesis, crystallization and preliminary X-ray diffraction results for a seven-base-pair tRNA^{Ser} acceptor-stem helix are presented here. Diffraction data were collected to 1.8 Å, applying synchrotron radiation and cryogenic cooling. The crystals belong to the monoclinic space group *C*2, with unit-cell parameters a = 36.14, b = 38.96, c = 30.81 Å, β = 110.69°.

1. Introduction

In the elongation cycle of protein biosynthesis, aminoacyl-tRNAs are carried to the ribosome by the elongation factor Tu. The ternary complex (aminoacyl-tRNA–EF-Tu–GTP) binds to the ribosomal A-site and the bound GTP is hydrolyzed to GDP and phosphate; EF-Tu–GDP then dissociates from the ribosome. The aminoacyl-tRNA at the A-site accepts the growing polypeptide and then is translocated to the ribosomal P-site. This cycle is repeated until a termination signal indicates the end of the protein to be synthesized.

However, there is one exception: the selenocysteine-specific UGA suppressor tRNA^{Sec} is not recognized by EF-Tu, but has its own elongation factor SELB, which specifically binds this tRNA and carries it to the ribosome (Forchhammer *et al.*, 1989; Förster *et al.*, 1990; Leinfelder *et al.*, 1988; Rother *et al.*, 2000). Prior to this, tRNA^{Sec} is aminoacylated with serine by seryl-tRNA synthetase and is then converted to selenocysteinyl-tRNA^{Sec} by an enzymatic process. Thus, selenocysteinyl-tRNA^{Sec} is generated by a substitution of the hydroxyl group of the tRNA-bound serine by a selenol group (Forchhammer, Boesmiller *et al.*, 1991; Forchhammer, Leinfelder *et al.*, 1991; Forchhammer & Böck, 1991). The cellular machinery for protein synthesis therefore necessitates a dual role for the tRNA$^{Ser/Sec}$ identity elements.

On the one hand, tRNA^{Sec} possesses the identity elements required by seryl-tRNA synthetase and has to be similar to the serine-specific tRNA isoacceptors (Sprinzl *et al.*, 1998). The aminoacyl domains of both tRNA^{Ser} and tRNA^{Sec} carry identity elements for aminoacylation with serine-tRNA synthetase (Schimmel, 1987), which is a class 2 synthetase (Eriani *et al.*, 1990). The structure of tRNA^{Ser} in complex with the aminoacyl-tRNA synthetase has been solved to 2.9 Å resolution (Biou *et al.*, 1994). However, since no electron density could be observed for the 3′ and 5′ ends of the aminoacyl domain in the complex, the current analysis of the isolated microhelices, which are identical in sequence to the complexed aminoacyl domain except for the 7–66 base pair, may provide further structural insights, possibly also in concert with the complexed synthetase structure.

On the other hand, identity elements for EF-Tu *versus* SELB recognition distinguish between seryl-tRNA^{Ser} and selenocysteinyl-tRNA^{Sec}. The regions responsible for SELB recognition and EF-Tu rejection are located in the aminoacyl stem and T-stem of tRNA^{Sec}. Prokaryotic tRNA^{Sec} possesses an eight-base-pair acceptor stem, in contrast to elongator tRNAs, which have a seven-base-pair acceptor stem, while both possess a five-base-pair T-stem. This leads to an '8/5'

model in tRNA^{Sec}, which results in an unusual 13-base-pair helix, in contrast to the '7/5' 12-base-pair model in tRNA^{Ser} (Leibundgut *et al.*, 2005) and all other prokaryotic elongator tRNAs. In order to analyse the structural (dis)similarities of tRNA^{Ser} and tRNA^{Sec} aminoacyl domains which distinguish between SELB/EF-Tu recognition, but govern the common recognition by serine-tRNA synthetase, we report the crystallization and X-ray diffraction data of a tRNA^{Ser} microhelix. We have already reported the crystallization of suppressor tRNA^{Sec} eight-base-pair aminoacyl stem (Förster *et al.*, 1999). As no structural data could be reported to date, further crystallization experiments on this microhelix have been initiated.

Here, we present the initial crystallographic data of the elongator tRNA^{Ser} seven-base-pair acceptor-stem helix. We anticipate that this will advance the understanding of the subtle structure–function relationships governing the incorporation of unusual amino acids, a topic of acute interest for the generation of novel proteins (Hendrickson *et al.*, 2004).

2. Materials and methods

2.1. RNA synthesis and purification

Two RNA oligonucleotides with sequences 5′-GGAGAGA-3′ and 5′-UCUCUCC-3′ were synthesized on an Applied Biosystems 394 DNA/RNA synthesizer by solid-phase phosphoramidite chemistry with the following RNA phosphoramidites: 5′-DMT-2′-tBDMS-rA(bz)-3′-CEP, 5′-DMT-2′-tBDMS-rG(ib)-3′-CEP, 5′-DMT-2′-tBDMS-rC(bz)-3′-CEP and 5′-DMT-2′-tBDMS-rU-3′-CEP (from Proligo, ChemGenes or of our own synthesis). ChemGenes or Proligo CPG 500A columns were packed and used for synthesis on the 1 µmol scale using the DMT-on strategy. Deprotection took place at 338 K with 40% aqueous methylamine for 20 min. After this step, RNA strands were lyophilized. The pellets were resuspended in 150 µl DMSO, 75 µl TEA and 200 µl TEA–HF for 2 h at 338 K. HPLC purification of the DMT-on product was performed with a 10 ml 15 RPC column from Amersham Biosciences. To remove the DMT group, the lyophilized DMT-on fractions were resuspended in 50 µl 80% acetic acid and incubated for 1 h at 323 K. The pH was adjusted with 3 *M* sodium acetate pH 6.5 and the product was again purified by HPLC. RNA was then desalted by G-10 column chromatography. The purity of the RNA product was verified by analytical RP-HPLC. The HPLC buffers were the following: *A*, 50 m*M* TEA acetate pH 7.0; *B*, 80% acetonitrile in 50 m*M* TEA acetate pH 7.0. The amount of RNA was determined by UV absorption (Sproat *et al.*, 1995).

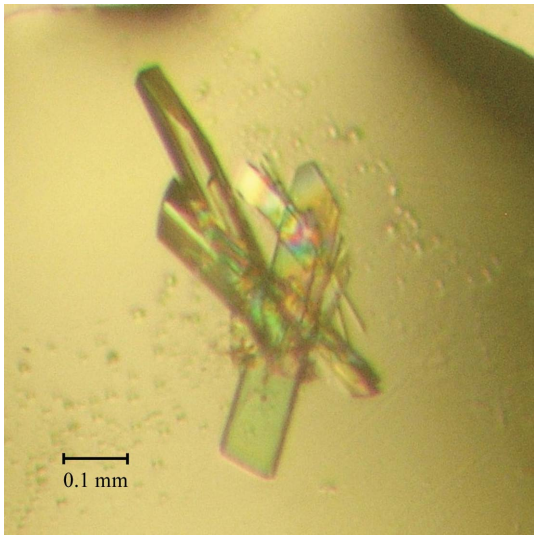

Figure 1
Crystals of the tRNA^{Ser} acceptor-stem helix grown under the optimized conditions described in the text.

2.2. Hybridization of RNA and crystallization

The two complementary strands 5′-GGAGAGA-3′ and 5′-UCUCUCC-3′ were hybridized in water at a concentration of 0.5 m*M* each for the formation of the tRNA^{Ser} microhelix. Heating to 363 K was followed by slow cooling to room temperature for several hours. The resulting tRNA^{Ser} duplex was used for all the following crystallization experiments.

Screening of crystallization conditions was performed by the sitting-drop vapour-diffusion method, applying the Natrix formulation from Hampton Research (CA, USA). For the initial crystallization trials, 1 µl 0.5 m*M* tRNA^{Ser} duplex in water was mixed with 1 µl crystallization buffer and sitting drops were equilibrated at 294 K against 80 µl reservoir solution in 96-well CrystalQuick Lp plates (Greiner Bio-One, Germany). Small crystals were obtained within 3–4 weeks under various crystallization conditions with lithium sulfate as precipitant. Crystallization conditions were further optimized and the final crystallization conditions were 50 m*M* sodium cacodylate pH 6.0, 15 m*M* magnesium sulfate and 1.8 *M* lithium sulfate. Under these conditions, crystals for X-ray measurements were obtained using the hanging-drop vapour-diffusion technique in 24-well Linbro Plates (ICN Biomedicals Inc., Ohio, USA). 1 µl 0.5 m*M* tRNA^{Ser} duplex in water was mixed with 1 µl reservoir solution and this mixture was equilibrated against 1 ml reservoir solution at 294 K. Crystals appeared after three weeks and grew to approximate dimensions of 0.4 × 0.1 × 0.05 mm (Fig. 1).

2.3. Crystallographic data collection and evaluation

X-ray diffraction data were collected at the ELETTRA synchrotron in Trieste on X-ray diffraction beamline 5.2R. Prior to data collection, crystals were transferred to a cryoprotectant solution and subsequently flash-frozen in liquid nitrogen. The cryoprotectant solution contained 50 m*M* sodium cacodylate pH 6.0, 15 m*M* magnesium sulfate, 1.8 *M* lithium sulfate and 20%(*v*/*v*) glycerol. A high-resolution data set (80–1.8 Å) was collected at a wavelength of 0.9 Å and at a temperature of 100 K. Data processing, the derivation of the space group and determination of the unit-cell parameters were performed with the *HKL*2000 package (Otwinowski & Minor, 1997).

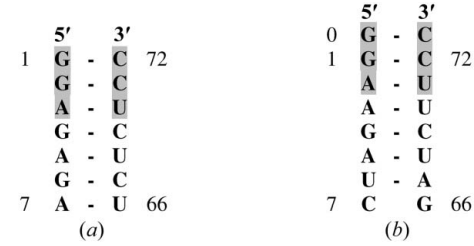

Figure 2
Comparison of the sequences of (*a*) tRNA^{Ser} and (*b*) tRNA^{Sec} acceptor-stem helix (the numbering of the nucleotides follows the nomenclature of Sprinzl *et al.*, 1998). These helices are homologous only in the first three base pairs (highlighted in grey), but differ in the rest of the sequence and also in length.

Table 1
Data-collection and processing statistics.

Values in parentheses correspond to the highest resolution shell.

Beamline	ELETTRA 5.2R
Wavelength (Å)	0.900
Space group	*C*2
Unit-cell parameters (Å, °)	a = 36.14, b = 38.96, c = 30.81, β = 110.69
Matthews coefficient V_M (Å^3 Da^{-1})	2.31
RNA duplexes per asymmetric unit	1
Solvent content† (%)	59
Measured reflections	11162
Unique reflections	3677
Resolution range (Å)	80.0–1.80 (1.83–1.80)
Completeness (%)	99.1 (100)
Multiplicity (%)	3.0 (2.7)
R_{merge}‡ (%)	6.6 (23.2)
Average $I/\sigma(I)$	14.9 (2.2)

† Estimated with the average partial specific volume calculated for RNA by Voss & Gerstein (2005). ‡ $R_{merge} = \sum_{hkl}\sum_i |I_i(hkl) - \langle I(hkl)\rangle| / \sum_{hkl}\sum_i I_i(hkl)$, where $I_i(hkl)$ and $\langle I(hkl)\rangle$ are the observed individual and mean intensities of a reflection with the indices hkl, respectively, $\sum_i$ is the sum over the individual measurements of a reflection with the indices hkl and $\sum_{hkl}$ is the sum over all reflections.

3. Results and discussion

3.1. Crystallization

Several serine-specific tRNA isoacceptors have been identified (for a compilation of sequences see Sprinzl *et al.*, 1998). In order to elucidate the minimal required differences in recognition elements between tRNA^{Ser} and tRNA^{Sec} in *Escherichia coli*, we selected a tRNA^{Ser} acceptor-stem helix (5′-$G_1G_2A_3G_4A_5G_6A_7$-3′/5′-$U_{66}C_{67}$-$U_{68}C_{69}U_{70}C_{71}C_{72}$-3′) that has a three-base-pair homology with the corresponding sequence of the selenocysteine-specific tRNA^{Sec} (Fig. 2).[1] The crystals of this tRNA^{Ser} microhelix appeared after 21 d at 294 K with 50 m*M* sodium cacodylate, 15 m*M* magnesium sulfate, 1.8 *M* lithium sulfate as precipitant at pH 6.0 and reached dimensions of 0.4 × 0.1 × 0.05 mm (Fig. 1).

3.2. Crystallographic data

The tRNA^{Ser} acceptor-stem helix crystallizes in the monoclinic space group *C*2, with unit-cell parameters a = 36.14, b = 38.96, c = 30.81 Å, β = 110.69°. We calculated a Matthews coefficient (Matthews, 1968) of 2.31 Å^3 Da^{-1}, which corresponds to one molecule of the helix per asymmetric unit (Table 1). Compared with the unit-cell parameters of the selenocysteine-tRNA^{Sec} acceptor-stem helix, the data clearly differ (Förster *et al.*, 1999). The difference in crystallization conditions and crystal morphology can be explained by the fact that tRNA^{Ser} acceptor stem is a seven-base-pair microhelix, as opposed to tRNA^{Sec}, which is an eight-base-pair microhelix with a different sequence except for a homology in the first three base pairs. The differences in structure and length of the two tRNA acceptor-stem helices obviously represent features of biological relevance. They contain the minimal consensus sequence for synthetase recognition and the length of the helix presents features relevant to interaction with EF-Tu or SELB.

[1] It is noteworthy that another tRNA^{Ser} acceptor-stem helix sequence (5′-$G_1G_2A_3A_4G_5U_6G_7$-3′/5′-$C_{66}G_{67}C_{68}U_{69}U_{70}C_{71}C_{72}$-3′) has an even higher homology with tRNA^{Sec}. However, initial experiments with this sequence (not described in this report) yielded crystals that showed only poor X-ray diffraction.

Diffraction data for the tRNA^{Ser} aminoacyl stem were collected to 1.8 Å and processed in the resolution range 80.0–1.8 Å. The overall R_{merge} is 6.6% (Table 1). Molecular-replacement calculations are presently in progress. Since there are no coordinates available of comparable tRNA^{Ser} microhelices, a variety of models are currently being tested, ranging from small oligonucleotide structures such as the tRNA^{Ala} acceptor stem 7-mer (PDB code 434d) to the corresponding region of native tRNAs such as the tRNA^{Phe} structure (PDB code 1ehz).

Most recently, the crystal structure of SELB, the selenocysteinyl-tRNA-specific elongation factor, was solved (Leibundgut *et al.*, 2005). This X-ray structure revealed a binding pocket which most probably accommodates the aminoacyl stem and T-stem of tRNA^{Sec} and possesses two positively charged amino acids in the vicinity of the selenol group. Further insights might be gained by docking experiments with tRNA^{Ser} and tRNA^{Sec} microhelix structures as well as by cocrystallization experiments. In summary, these investigations might help to understand why seryl-tRNA^{Ser} binds to the aminoacyl-binding pocket of EF-Tu (Nissen *et al.*, 1995) like all other elongator tRNAs, but selenocysteinyl-tRNA^{Sec} interacts exclusively with SELB.

This work was funded in the RiNA network for RNA technologies by the Federal Ministry of Education and Research, the City of Berlin and the European Regional Development Fund. We gratefully acknowledge the ELETTRA synchrotron, Trieste for providing beamtime and the European Union, Fonds der Chemischen Industrie (Verband der Chemischen Industrie e.V.) and the National Foundation for Cancer Research, USA for additional support.

References

Biou, V., Yaremchuk, A., Tukalo, M. & Cusack, S. (1994). *Science*, **263**, 1404–1410.
Eriani, G., Delarue, M., Poch, O., Gangloff, J. & Moras, D. (1990). *Nature (London)*, **347**, 203–206.
Forchhammer, K. & Böck, A. (1991). *J. Biol. Chem.* **266**, 6324–6328.
Forchhammer, K., Boesmiller, K. & Böck, A. (1991). *Biochimie*, **73**, 1481–1486.
Forchhammer, K., Leinfelder, W. & Böck, A. (1989). *Nature (London)*, **342**, 453–456.
Forchhammer, K., Leinfelder, W., Boesmiller, K., Veprek, B. & Böck, A. (1991). *J. Biol. Chem.* **266**, 6318–6323.
Förster, C., Eickmann, A., Schubert, U., Hollmann, S., Müller, U., Heinemann, U. & Fürste, J. P. (1999). *Acta Cryst.* D**55**, 664–666.
Förster, C., Ott, G., Forchhammer, K. & Sprinzl, M. (1990). *Nucleic Acids Res.* **18**, 487–491.
Hendrickson, T. L., de Crecy-Lagard, V. & Schimmel, P. (2004). *Annu. Rev. Biochem.* **73**, 147–176.
Leibundgut, M., Frick, C., Thanbichler, M., Böck, A. & Ban, N. (2005). *EMBO J.* **24**, 11–22.
Leinfelder, W., Zehelein, E., Mandrand-Berthelot, M. A. & Böck, A. (1988). *Nature (London)*, **331**, 723–725.
Matthews, B. W. (1968). *J. Mol. Biol.* **33**, 491–497.
Nissen, P., Kjeldgaard, M., Thirup, S., Polekhina, G., Reshetnikova, L., Clark, B. F. & Nyborg, J. (1995). *Science*, **270**, 1464–1472.
Otwinowski, Z. & Minor, W. (1997). *Methods Enzymol.* **276**, 307–326.
Rother, M., Wilting, R., Commans, S. & Böck, A. (2000). *J. Mol. Biol.* **299**, 351–358.
Schimmel, P. (1987). *Annu. Rev. Biochem.* **56**, 125–158.
Sprinzl, M., Horn, C., Brown, M., Ioudovitch, A. & Steinberg, S. (1998). *Nucleic Acids Res.* **26**, 148–153.
Sproat, B., Colonna, F., Mullah, B., Tsou, D., Andrus, A., Hampel, A. & Vinayak, R. (1995). *Nucleosides Nucleotides*, **14**, 255–273.
Voss, N. R. & Gerstein, M. (2005). *J. Mol. Biol.* **346**, 477–492.